

# Polarimetric Effects in Non-polarimetric Imaging

Russel P. Kauffman\*<sup>1a</sup> and Michael Gartley<sup>b</sup>

<sup>a</sup> Lockheed Martin Information Systems and Global Services, P.O. Box 8048, Philadelphia PA, 19101;

<sup>b</sup> Digital Imaging and Remote Sensing Laboratory, Chester F. Carlson Center for Imaging Science, Rochester Institute of Technology, 54 Lomb Memorial Drive, Rochester, NY 14623-5604

## ABSTRACT

Radiative transfer is commonly modeled as the propagation of unpolarized radiation. More accurate approaches utilizing polarimetric quantities are usually only applied to sensors that purposefully discriminate polarimetric information. In this paper, we examine the effect on fidelity of utilizing polarimetric radiative transfer modeling for non-polarimetric sensors. We show that if the primary irradiance on a scene is significantly polarized (such as sky irradiance) then polarimetric radiative transfer modeling is warranted and provides a significant increase in fidelity. We demonstrate this effect by performing target detection of shadowed man-made objects in real and simulated imagery.

**Keywords:** Polarimetry, radiative transfer

## 1. INTRODUCTION

In this section we review the basics of polarized reflective radiometry and introduce notation. Radiative transfer is commonly modeled as the propagation of unpolarized radiation. Most sensors are insensitive to polarization. (However, a sensor that is designed to be unpolarized may still have unintended polarization sensitivity.) In reflective radiometry, the main radiation source, direct solar radiation, is almost completely unpolarized. If both the radiation source and the sensor are unpolarized then the effects of the polarization of the material's reflecting properties are zero. For an unpolarized sensor then, polarization effects arise only when both the material and the downwelling (skydome) radiance are polarized.

If polarizing effects are neglected, the reflected downwelling radiance can be written

$$L_{dr} = \int f(\theta_i, \theta_r) L_d(\theta_i) d\Omega_p, \quad \text{Eq. [1]}$$

where  $L_d(\theta_i)$  is the downwelling radiance,  $f(\theta_i, \theta_r)$  is the BRDF as a function of the directions of the incident radiation ( $\theta_i$ ) and that of the reflected radiation ( $\theta_r$ ), and  $d\Omega_p$  is the differential projected solid angle for the incident radiation:

$$d\Omega_p = d\Omega \cos \theta = \cos \theta_i \sin \theta_i d\theta_i d\phi_i. \quad \text{Eq. [2]}$$

In Eq. 1, we have suppressed the wavelength dependence of the radiances and the BRDF.

When polarization is important, Eq. [1] becomes a matrix equation for the reflected Stokes vector:

$$\mathbf{S}_{dr} = \int \mathbf{M}(\theta_i, \theta_r) \mathbf{S}_d(\theta_i) d\Omega_p, \quad \text{Eq. [3]}$$

in which  $\mathbf{M}(\theta_i, \theta_r)$  is the Mueller matrix describing the reflection and  $\mathbf{S}_d(\theta_i)$  is the Stokes vector of the downwelling radiance, and again, wavelength dependence has been suppressed. For those unfamiliar to polarized radiometry, we note that the unpolarized BRDF is the 00 component of the Mueller matrix,

$$M_{00}(\theta_i, \theta_r) = f(\theta_i, \theta_r). \quad \text{Eq. [4]}$$

If the sensor is unpolarized, only the 0th component of the Stokes vector is of interest, and we have

---

\*russel.p.kauffman@lmco.com; phone 1 610 531-1768

$$S_{odr} = \int \mathbf{M}_0(\theta_i, \theta_r) \mathbf{S}_d(\theta_i) d\Omega_p, \quad \text{Eq. [5]}$$

where  $\mathbf{M}_0$  is the zeroth row of the Mueller matrix  $\mathbf{M}$ . In general,

$$\mathbf{M}_0 \mathbf{S}_d = M_{00} S_{d0} + M_{01} S_{d1} + M_{02} S_{d2} + M_{03} S_{d3} \neq M_{00} S_{d0}. \quad \text{Eq. [6]}$$

The primary goals of this paper are to investigate the deviation between the two sides of this inequality, or rather between their respective integrals over projected solid angle, and determine under what circumstances they may be important.

## 2. THEORY

Under clear sky conditions with primarily Rayleigh scattering in the atmosphere, and ignoring multiple scattering effects and elliptical polarization, the degree of polarization (DOP) and the azimuth angle of the polarization (AOP) of skylight can be computed, with reasonable accuracy as a function the altitude and azimuth of the sun and those of the point of observation [7,8]. From the figures and formulas in Ref. 7 and 8, we see that there are portions of the sky that are nearly horizontally polarized and portions that are nearly vertically polarization.

Surface reflection changes the state of polarization of the incident unpolarized light in such a way that the AOP of the reflected light will be vibrating in a plane that is parallel to the surface of the material. For horizontal surfaces, horizontally polarized sections of the sky are reflected strongly, whereas vertically polarized sections are not. For this reason, we expect that the effects we are predicting will have a positive effect on the sensed radiance when the reflected sky is horizontally polarized, and a negative effect on the sensed radiance when the sky is vertically polarized.

In conventional material detection/characterization approaches, the reflecting surface is assumed to be diffuse. Under this assumption, Eq. [1] for the reflected downwelling radiation takes the form

$$L_{dr} = f \int L_d(\theta_i) d\Omega_p. \quad \text{Eq. [7]}$$

We propose to use a simplified model of the Mueller matrix for a reflecting surface. We will assume that the diffuse component of the reflectance is depolarizing and Lambertian and that only the first-surface reflection is polarized. Under this model, Eq. [3], takes the form

$$S_{odr} = f_d \int S_{od}(\theta_i) d\Omega_p + \mathbf{R}_0(\theta_s) \mathbf{S}_d(\theta_g), \quad \text{Eq. [8]}$$

where the glint direction is denoted by  $\theta_g$ . For a dielectric surface, the Mueller matrix has no terms that mix  $S_2$  with the other components,

$$\mathbf{R}_0(\theta_s) \mathbf{S}_d(\theta_g) = R_{00}(\theta_s) S_{d0}(\theta_g) + R_{01}(\theta_s) S_{d1}(\theta_g). \quad \text{Eq. [9]}$$

The two non-zero Mueller-matrix components can be computed from the Fresnel reflective coefficients for the surface.

## 3. APPROACH

To determine the effect of the inclusion/omission of polarimetric modeling, we consider the problem of detecting a certain paint when shadowed. Our “target” is a car with three different paint colors. We consider two detection metrics: 1) the ratio of the blue signal (wavelength 450 nm) to the red signal (wavelength 650 nm) and 2) the spectral angle for the visible region. Figure 2 shows a simulation of our target, with the exploited region highlighted. Specifically, we consider the spectral angle between the following modeled radiances: 1) diffuse model and unpolarized BRDF; 2) diffuse model and polarized BRDF; 3) polarized and unpolarized BRDF models. Likewise, we compute the red-blue ratio for all three of these models.



Figure 1. Car in shade

#### 4. RESULTS

For our simulations, we have chosen two collection conditions, distinguished from each other by the polarization of the piece of sky that is in the glint direction. For position 1, the skylight in the glint direction is horizontally polarized. For position 2, the skylight in the glint direction is vertically polarized.

Figures 2-4 show the at-aperture spectral radiance for our three paint colors for the glint direction in positions 1 and 2, respectively. We note first that there is a substantial difference between the diffuse and specular models, even if polarizing effects are neglected. Clearly, the angular dependence of the reflectance is important. Secondly, we note that the modeled results using the pBRDF and the unpolarized BRDF are visibly different. When the reflected sky is horizontally polarized, the polarized modeling produces a larger result than the unpolarized model. When the reflected sky is vertically polarized, the polarized model produces a smaller result than the unpolarized model. These effects are due to the preferential reflection that the horizontal surface gives to horizontally polarized light.

These differences are reflected in our two detection metrics, as shown in Table 1. Table 1 shows sizable differences between the modeled at aperture radiance for the unpolarized and polarized BRDF models. When the sky glint is horizontally polarized, the pBRDF model shows a larger red-blue ratio than the unpolarized BRDF model, whereas when the sky is vertically polarized, the pBRDF red-blue ratio is reduced compared to the unpolarized result.

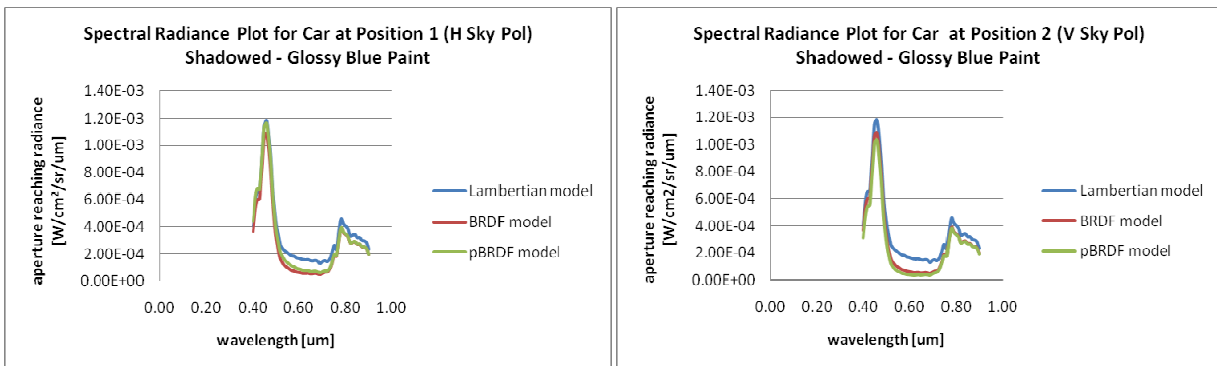


Figure 2: Spectral radiance plots for blue paint

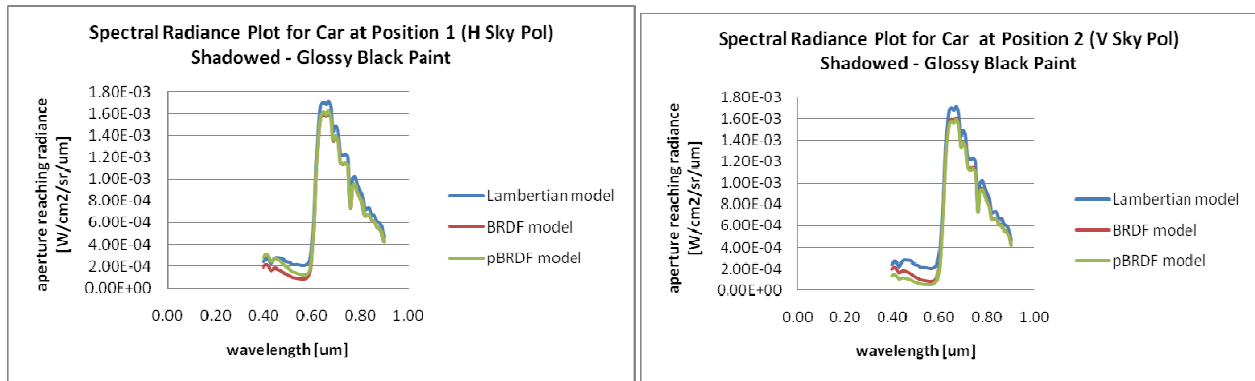


Figure 3: Spectral radiance plots for black paint

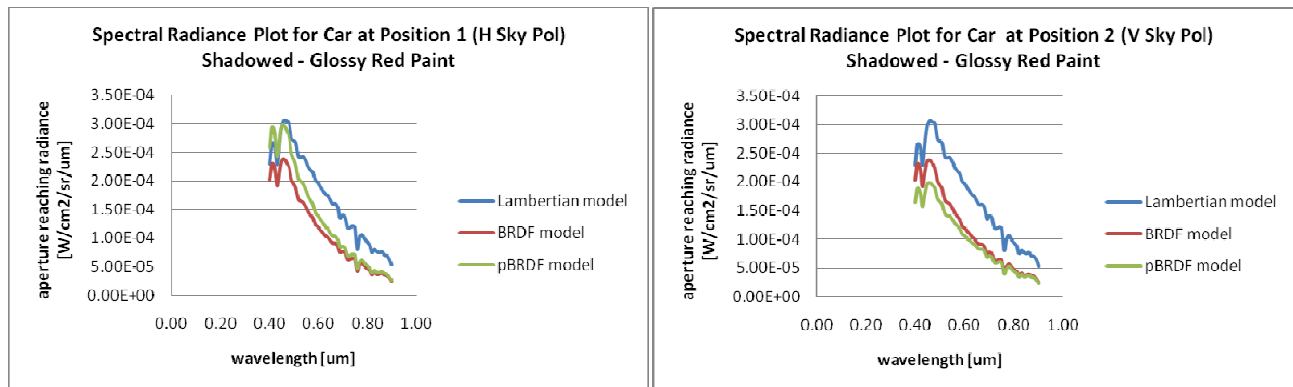


Figure 4: Spectral radiance plots for red paint

Table 1: Simulated results for shadowed targets.

Paint Color	Glint Polarization	Spectral Angle (°)			Red/Blue		
		Diffuse to BRDF	Diffuse to pBRDF	BRDF to pBRDF	Diffuse	BRDF	pBRDF
Red	Horizontal	7.1	6.1	1.1	6.1	8.7	5.8
Red	Vertical	7.4	9	1.6	6.1	8.7	13.1
Blue	Horizontal	0.9	1.7	1.6	0.13	0.048	0.061
Blue	Vertical	0.9	1.7	1.3	0.13	0.048	0.038
Black	Horizontal	3.1	3.8	0.7	0.557	0.402	0.365
Black	Vertical	3.3	2.5	0.8	0.557	0.401	0.439

Table 2: Simulated results for sunlit targets.

Paint Color	Glint Polarization	Spectral Angle (°)			Red/Blue		
		Diffuse to BRDF	Diffuse to pBRDF	BRDF to pBRDF	Diffuse	BRDF	pBRDF
Red	Horizontal	13.5	12.3	1.3	10.1	33.1	24.3
Red	Vertical	13.8	15.2	1.5	10.1	33.1	44
Blue	Horizontal	2.2	1.6	0.7	0.215	0.045	0.049
Blue	Vertical	2.2	2.6	0.5	0.215	0.045	0.041
Black	Horizontal	2.5	3.4	0.9	0.919	0.759	0.706
Black	Vertical	2.6	1.8	0.8	0.919	0.759	0.802

## 5. CONCLUSION

Our results show that polarizing effects need to be included for high-precision modeling of specular surfaces reflecting polarized light, even when the detecting sensor is unpolarized. When the paint targets that we have considered are shadowed, the inclusion of polarization makes as much as a 50% difference in the red-blue band ratio. The effects are smaller for sunlit targets, on the order of 10% in the red-blue band ratio.

## REFERENCES

- [1] Gartley, M.G., Brown, S.D., Goodenough, A.A., Sanders, N.J., and Schott, J.R., "Polarimetric scene modeling in the thermal infrared," Proc. SPIE 6682, 66820C (2007).
- [2] Gartley, M.G. and Basener W, "Topological Anomaly Detection Performance with Multispectral Polarimetric Imagery," Proc. SPIE 7334, 73341O (2009).
- [3] Matchko, R. and Gerhart, G., "Polarization azimuth angle in daylight scenes," Opt. Eng. 44, 028001 (2005).
- [4] Devaraj, C., Brown, S., Messinger, D., A. Goodenough and D. Pogorzala, "A framework for polarized radiance signature prediction for natural scenes," Proc. SPIE 6565, 65650Y (2007).